Mar Geophys Res
DOI 10.1007/s11001-010-9091-z

ORIGINAL RESEARCH PAPER

Effects of sea states on seafloor compliance studies

Jui-Hsien Wang · Wu-Cheng Chi · R. Nigel Edwards · Eleanor C. Willoughby

Received: 2 November 2009 / Accepted: 24 June 2010

Abstract Gas hydrates affect the bulk physical properties of marine sediments, in particular, elastic parameters. Shear modulus is an important parameter for estimating the distribution of hydrates in the marine sediments. However, S-wave information is difficult to recover without proper datasets. Seafloor compliance, the transfer function between pressure induced by surface gravity waves and the associated seafloor deformation, is one of few techniques to study shear modulus in the marine sediments. The coherence between recorded time series of displacement and pressure provides a measure of the quality of the calculated transfer function, the seafloor compliance. Thus, it is important to understand how to collect high coherence datasets. Here we conducted a 10-month pilot experiment using broadband seismic sensors and differential pressure gauges. We found that data collected in shallow water depth and during rough seas gave high coherence. This study is the first time long-term data sets have been employed to investigate seafloor compliance data quality and its dependence on sea state. These results will help designing future large-scale compliance experiments to study anomalously high shear moduli associated with the presence of gas hydrate or cold vents, or alternatively anomalously low shear moduli, associated with partial melt and magma chamber.

J.-H. Wang · W.-C. Chi (✉)
Institute of Earth Sciences, Academia Sinica, Taipei, Taiwan, ROC
e-mail: wchi@gate.sinica.edu.tw

J.-H. Wang
Department of Mechanical Engineering, National Taiwan University, Taipei, Taiwan, ROC

R. Nigel Edwards · E. C. Willoughby
Department of Physics, University of Toronto, Toronto, Canada

Keywords Seafloor compliance · Coherence · Sea-state · Gas hydrate

Introduction

Methane hydrates are ice-like crystalline solids formed from a mixture of water and methane molecules. Most hydrates have been found in deep ocean sediments where there is a sufficient supply of methane and where pressure and temperature ranges between 0.2-5 MPa and 0–25°C, respectively (Kvenvolden and McMenamin 1980; Fig. 1). The total mass of natural gas hydrate deposits has been estimated to range from 10^{18} to 10^{19} g (e.g. Milkov 2004; Kvenvolden 1988). Because one volume of hydrate can contain up to 164 volumes of free gas (Kvenvolden 1993), it stores energy densely. The hydrates and any free gas trapped below may provide a significant hydrocarbon resource in the future (Kvenvolden and McMenamin 1980; Kvenvolden 1993).

Methane hydrates are also viewed as a potential geohazard (Kvenvolden 1993), in terms of seafloor instability and global warming. Changes in the thickness of the gas hydrate stability zone (GHSZ) due to in situ pressure or temperature perturbations might change geotechnical properties of shallow marine sediments, thus influencing seafloor stability. Methane hydrate in marine sediments may form a significant global sink of methane, a gas that is about 20 times as effective a greenhouse gas as carbon dioxide. Variations in bottom water temperature or the position of sea level may influence the stability of hydrate, and in some cases, could result in the release of additional methane into the atmosphere and potentially influent climate (Kvenvolden and McMenamin 1980; Kvenvolden 1993). To study the potential influences of these processes,

Published online: 23 July 2010

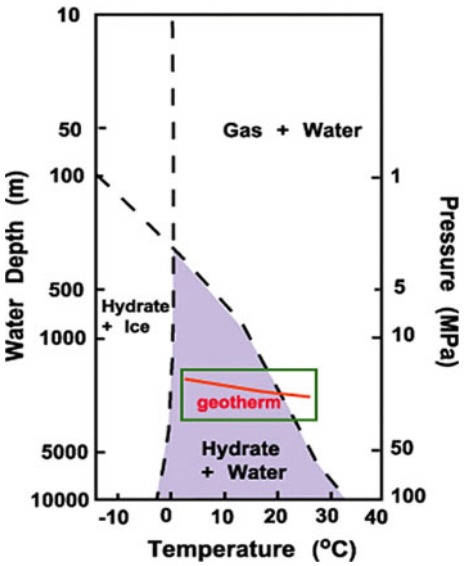

Fig. 1 Phase diagram of gas hydrate (modified from a figure at NOAA website: URL:http://oceanexplorer.noaa.gov/explorations/03windows/background/hydrates/media/fig1_phase_diagram.html). The green box represents the hydrostatic pressure condition and temperature condition (due to geothermal gradient) in shallow sediments under the seafloor. The intersect of the *red line* (geothermal gradient) and the phase boundary marks the location where hydrates are stable above and methane gas is stable below. This is where the bottom-simulating reflector (BSR) is located. See text for details

it is important to study the occurrence of gas hydrates in submarine environment. One of the techniques to study gas hydrate is seafloor compliance (Willoughby and Edwards 1997; Willoughby et al. 2000, 2008).

Seafloor compliance is a relatively novel technique to evaluate the subsurface shear modulus by using pressure exerted on the seafloor and the ground displacement. This method was pioneered in shallow water application by Yamamoto et al. (Yamamoto and Torii 1986; Trevorrow et al. 1989; Yamamoto et al. 1989), and then developed for deeper water cases by Crawford et al. (1991). The compliance is the transfer function between seafloor pressure and displacement as a function of frequency. The horizontal and vertical scale of the pressure field is set by the wavelength of the surface gravity waves. The pressure field amplitude and oceanic crustal elastic parameters, especially shear properties, determine the amplitude of the deformation (Crawford et al. 1991; Willoughby, 2003). Seafloor compliance is usually normalized by multiplying wave number of the source.

The pressure field on the deep seafloor can be generated by infragravity waves. Infragravity waves are wind-induced long periods (20–250 s) ocean waves. In the ocean, the radiation stresses of the infragravity waves increases with decreasing water depth (Longuet-Higgins and Stewart 1962). Such stress exerts pressures on the seafloor, and cause seismic ground motions in similar bands. According to Webb et al. (1991), infragravity waves are generated in the near shore region along the entire coastline of an ocean basin through nonlinear transfer of energy from short-period waves. Seismic signals induced by ocean waves in the infragravity bands have been documented (Rhie and Romanowicz 2004; Webb et al. 1991; Webb 2007).

To study seafloor compliance, it is necessary to use pressure and seismic data that are coherent, meaning that the local seismic signals are solely a response of local pressure perturbation. Thus, coherence studies are the first step before the data can be used for compliance studies. Estimating and correcting for the measurement uncertainty is one of the most critical but difficult and time consuming tasks for compliance analysis. This uncertainty is calculated using the number of time windows and the coherence between the pressure and acceleration signals. Ideally, the coherence should be very high (>0.95), or the majority of noise should be on only one of the channels (Crawford and Singh 2008). However, it is still not clear what kinds of sea state are best for generating high coherence datasets, due to lack of long term sea bottom instrument deployments. Such knowledge will be very helpful for designing seafloor compliance experiments in the future.

Once compliance data with high coherence (>0.95) are available, or if we have information on how much noise is on each channel, they can be inverted to yield the profile of shear modulus in the shallow oceanic crust (Crawford and Singh 2008; Yamamoto and Torii 1986; Crawford et al. 1991). Shear modulus is a parameter particularly sensitive to the amount of gas hydrates in the sediment pore spaces, and therefore can be used to assess hydrates in the hydrate stability zone (Willoughby and Edwards 1997). Here we report the results of first pilot study conducted in the western Pacific Ocean in deep ocean to study if we can collect high coherence datasets for a proposed seafloor compliance study. We have conducted such experiment to learn if it is possible to use this technique to study hydrate system offshore Taiwan in the future.

Hydrate studies offshore Taiwan

Several large scale marine experiments have improved dramatically our understanding of the crustal structures and the distribution of the hydrates offshore Taiwan (Liu et al. 2006, Chi et al. 1998; 2006; Chi and Reed 2008; McIntosh et al. 2005). Surface seismic reflection data can image hydrate formations through the presence of a bottom-simulating reflector, or BSR that is subparallel to the topography of the sea floor (Shipley et al. 1979). These seismic

reflectors are generated by the acoustic impedance contrast at the base of the gas hydrate stability zone between a free gas layer trapped beneath gas hydrate-containing sediments, typically several hundred metres below the seafloor. The increase in temperature with depth below the seafloor causes methane hydrate to become unstable and decompose, despite increasing pressure. As a result, the base of the methane hydrate defines a "phase boundary" that separates the stable gas hydrate above from a field of instability below. Because they are not structural reflectors, they can sometimes cut across reflectors generated by sediment layers (Tucholke et al. 1977; Shipley et al. 1979).

Reed et al. (1992) first identified a BSR offshore Taiwan and interpreted it as evidence of the presence of gas hydrates. Chi et al. (1998) have discussed additional evidence to argue that the BSR around southern Taiwan represents the base of the gas hydrate stability field, separating the hydrates from the underlying free gas. The BSR is widespread in areas of the accretionary prism composed of sediments scraped off of the Chinese continental margin and the Taiwan orogen, which may reflect high amounts of organic carbon in rapidly deposited terrigenous sediments. Recently, Liu et al. (2006) have derived a new BSR distribution map offshore Taiwan. All such studies show wide-spread BSRs in this region, and potentially there are large amount of hydrate-related hydrocarbon, including gases, occurred in the offshore region. Recent studies also found strong evidences of hydrates inside Okinawa Trough offshore NE Taiwan (Ning et al. 2009).

First Taiwan BBOBs program

Starting in 2001, Academia Sinica of Taiwan launched the first broadband ocean bottom seismology program in Taiwan. In 2004, broadband ocean bottom seismometers (OBSs), with flat instrument response up to 120 s, were built in collaboration with Woods Hole Oceanographic Institution, and then deployed from Sept 2006 to July 2007. Two OBSs (S002 and S004, Fig. 2) were recovered from seafloor depths of 1749 m and 4726 m, respectively (S002: 25°2′43.8″N, 123°7′39.36″E; S004: 22°20′43.8″N, 122°38′57.12″E). Locations of the OBS sites are shown in Fig. 2. The estimated sediment thickness at S002 is 300–400 m. They recorded ground motions and water pressure data on the seafloor for a duration of 10 months.

The pressure at the seafloor is recorded by a differential pressure gauge (DPG), made by the Marine EM Lab, Scripps Institution of Oceanography, following the prototype made by Cox et al. (1984). The DPG can record very broadband acoustic signals up to 1000 s. The vertical ground motion is recorded by a Guralp CMG-3TC sensor,

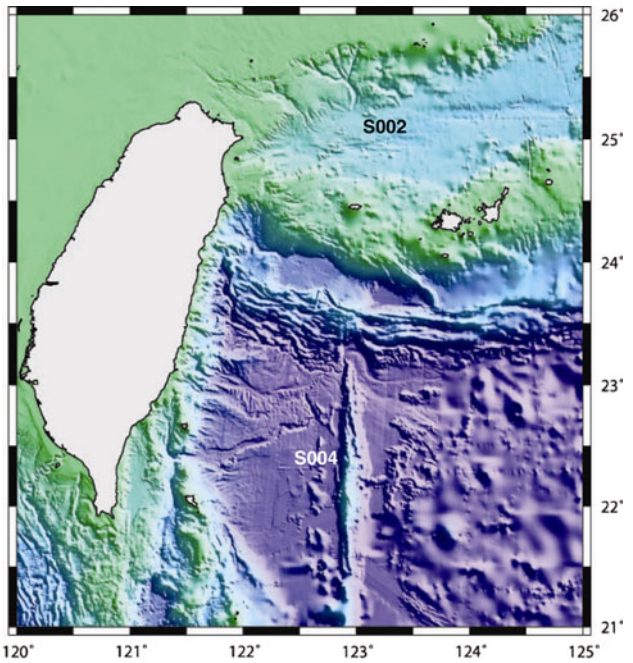

Fig. 2 Regional map of Taiwan, and ocean bottom seismometer (OBS) locations. The deepest water depth in this figure is about 5,000 m. Here we used the data collected by OBSs S002 and S004 for this study. S002 is located at shallow water region with a very thin sedimentary layer over basement. Most of the results of this study were derived from this site. S004 is located in deep water region

which has a flat response up to 120 s. The performance of this sensor is similar with the Guralp CMG-3T type but is altered to fit in the OBS system. The sensor is equipped with a gimbal system to level itself with an accuracy up to ± 2.5° once every week. The sampling rate is 20 sample per second (sps) for pressure channel and 40 sample per second for velocity channels. These data were recorded independently, although the pressure data were simultaneous recorded with the velocity measurement. All signals are digitized using a Q330 datalogger and then stored in 24-bit precision.

The performance of the broadband OBSs is good. During calm days, the recorded seismic signals are as quiet as land seismic stations (Lin et al. 2010). However, the microseisms and infragravity wave energies increase during the stormy days (Chi et al. 2010).

The 10-month deployment was originally designed for seismic studies (Kuo et al. 2009). However, here we have also used this dataset for a seafloor compliance study, which is usually applied jointly with seismic data to produce estimate of the total mass of a hydrate deposit. Willoughby and Edwards (1997) first adopted seafloor compliance methods for the resource evaluation of gas hydrates and have been employing the method for over a decade. Learning from their expertise, and with the newly

available dataset, we were able to conduct one of the first compliance studies in Asia. These dataset is unique in that, with the 10-month time series, we aimed to study in what kinds of sea-state and what water depths we can collect good waveforms for compliance studies. The experiences learned from this study will be important for siting of future compliance studies over hydrated sediments.

Data analyses

We will first describe the pressure spectra (forcing) collected during our experiment. Then we will study the velocity spectra (response), and the coherence in relation to sea-state. Finally, we will pick the best pressure and seismic datasets to derive the transfer function bounds, and then calculate the compliance function. Because our data are not located in the hydrated regions, it is out of our scope to derive the velocity profile and estimate concentrations of hydrates and gases in this work by inverting the compliance curve. However, our main contribution is showing that it is possible to use compliance to study hydrate in this region, and documenting and developing some criteria for designing future seafloor compliance experiences.

The deep-seafloor pressure power spectra of OBS site 002 (Fig. 3) shows a similar trend as previous studies done by Webb et al. (1991), although their data were collected from Atlantic Ocean. Energies are concentrating on two sides of the graph: the microseimic band and the infragravity band. The energetic microseimic peak in the waveband of

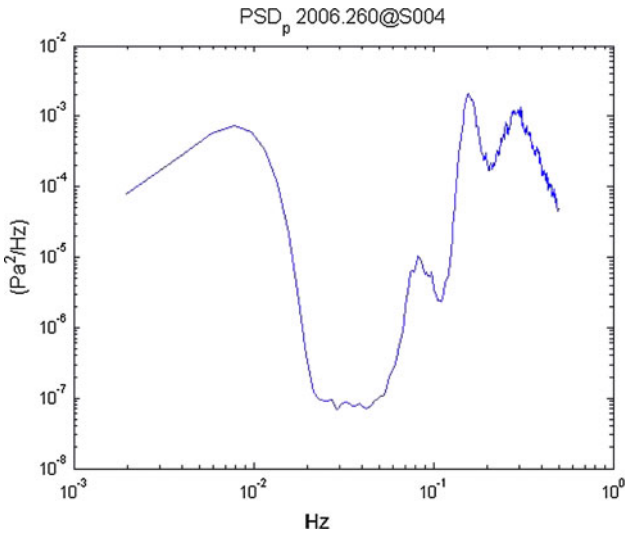

Fig. 3 Power spectral density of pressure recorded at site S004 for Julian day 260 of 2006. Even at a water depth of about 5 km, the DPG on the OBS recorded storm-induced pressure signals in the microseismic band, and wind and coast-line induced pressure signals in the gravity and infragravity waveband

0.1 to 1.0 Hz is mainly result from the propagation of the elastic waves with energy partitioned between the ocean and seafloor rocks depending on wave mode and frequency (Kibblewhite and Ewans, 1985). There is an obvious noise notch in which the spectrum drops 40–50 dB presented between 0.03 and 0.2 Hz. The low signal level in this band is probably because the hydrodynamic and acoustic scales are either too large (acoustic) or too small (hydrodynamic) for energy to easily coupled into propagating waves (Webb et al. 1991).

There is a sharp increase of the energy at frequencies below 0.03 Hz. The strong signal is mainly caused by the infragravity waves of this region. Infragravity waves obey the well-known dispersion relationship:

$$\omega^2 = gk \tan h(kh)$$

where ω is the frequency, g is the gravity constant, k is the wave number, and h is the water depth. Based on previous studies, waves with wavelengths between 0.5 and 2 times of the water depth are most likely to exert forces on the seafloor (Crawford et al. 1991). Therefore wave number $k = 2\pi/nH$, resulting in the cut-off frequency falls between 0.0211 and 0.0423 Hz, as $f_c = \sqrt{g/(2\pi nH)}$, $H = 1749$ m (at site S002), and $0.5 < n < 2$.

Both S002 and S004 OBSs had laid on the seafloor for nearly a year, recording a complete record of pressure and of seafloor displacement during the ever changing weather in west Pacific Ocean, including a typhoon passing almost right above the deployed sites (Chi et al. 2010). In addition, the wave conditions, wind conditions and the air pressure data near the deployed sites S002 and S004 are also available, enabling us to establish a unique, integrated seabed dataset with quantified weather and sea-state conditions.

To analyze this enormous dataset systematically, we have developed a standard examination procedure. Judging from the experience, earthquakes in this region with magnitude greater than 4.0 will induce uncorrelated ground motions and pressure waveforms, contaminating the signal quality. Waveforms in days with any Mw > 4.0 earthquakes with epicental distance <400 km, and Mw > 6 global earthquakes in the IRIS earthquake catalog were excluded from our compliance analysis. However, for simplicity, the coherence analyses were performed on the entire dataset.

The quality of the signal is also affected by the weather, and the condition of the sea surface. The weather data were recorded from the near-by Ishigaki Island provided by the Wave Information Department, Coastal Development Institute of Technology, Japan. The weather buoy was located at 24°20′34.08″N and 124°7′45.84″E, approximately 130 km away from OBS site S002 and 270 km away from OBS site S004. Due to the relatively long wavelength of infragravity wave and assuming the sea state does not

changes a lot spatially, we consider that the wave condition at buoy site is also representative for the OBS sites. Under this assumption, we have studied the influences on the data quality by several parameters such as wave height and wave period.

Data quality is expressed by the coherence of these data. Coherence, ranging from 0 to 1, quantifies the extent of how two series are related. After transforming our velocity into acceleration, we are able to calculate the coherence between the pressure series and the acceleration series. A high coherence implies that the ground motions are mostly induced by the pressure exerted on the seafloor in situ. In other words, the coherence can be treated as an indicator of the signal quality for compliance studies.

All raw data are stored in binary miniSEED (SEED: The Standard for the Exchange of Earthquake Data) format and are converted into standard SAC (Seismic Analysis Code) files. Each daily record is separated into 169 segments by 512-s Hann window with 25% overlap. We have performed instrument response correction and remove mean as pre-processing procedures. The power spectral densities are calculated for both pressure and acceleration waveforms and then coupled to obtain the coherence of the dataset. According to Crawford (2000), the compliance signal can be estimated with PSDs of pressure and acceleration as follows:

$$\eta(\omega) \equiv \frac{k(\omega))\hat{\gamma}_{pa}(\omega)}{\omega^2}\sqrt{\frac{|\hat{S}_a(\omega)|}{|\hat{S}_p(\omega)|}}$$

Where η is the estimated compliance, k is the wave number, $\hat{\gamma}_{pa}$ is the coherence, $\hat{S}_a$ is the power spectral density of acceleration signal and $\hat{S}_p$ is the power spectral density of pressure signal. This equation assumes that all noises are on the acceleration channel, which is generally true at the deep seafloor. However, there might be exceptions, especially at the low frequency bands. The effects of such assumption and their remedy are discussed in detail in the appendix of Crawford and Singh (2008).

Sea-state and coherence

It is assumed that changes in sub-seafloor shear moduli are small and occur over long time periods, so the seafloor compliance signal at a given location should be stable. Therefore, previous studies deployed instruments at one site for 2–3 days or even less (Crawford 2000; Willoughby 2003). Such short term studies mean the researchers can move the instruments to cover more sites. On the other hand, our OBS system is settled on the seafloor and retrieved 10 months later. This provides us a good opportunity to study influences of sea state on coherence. Through two deployments, each lasted for a day, Willoughby (2003) looked at the effect of weather on seafloor compliance data quality with 17 day-long deployments, employing a gravitmeter (as an accelerometer) and a differential pressure gauge. She found that higher coherence data were recorded under calmer seas, judging from the decreasing coherence at the day with significant swell and windy condition. With the abundance weather data, we are able to analyze the effect of wind and wave conditions more systematically. We found a strong positive correlation between the significant wave height and the data quality, as shown in Fig. 4a, which shows positive correlation between these two time series. The significant wave height in our deployed site generally lies within 1.0 m, yet days with ShanShan typhoon (Julian date:2006.257 to 2006.259, translating to about days 14–16 in Fig. 4a) passing by are showing much greater wave height, and high coherence (Fig. 4b). Thus, the coherence in infragravity band is roughly correlated with the significant wave height. The 2 days when Typhoon ShanShan passed over the OBS (2006.259 and 2006.260) gave highest coherence with significant wave heights of 3.364 m and 1.525 m, respectively. The coherence usually decreases as the significant wave height decreases. However, we also found some calm days sometimes giving relatively high coherence (Fig. 4b). Thus the effect of significant wave height does not always dominate coherence. To show the results in different way, we have also plotted Fig. 5, which also shows correlation between the significant wave heights and the coherence function for the infra-gravity bands. With the high coherence data, we are ready to use the waveforms to derive the compliance curve.

Compliance curve derived from date 2006.259 data

One of the major applications of the compliance technique is to obtain the shear modulus of the region, and estimate the gas hydrate concentration. We will apply the best data to perform the following analysis. The compliance signal is estimated through the power spectral densities of both pressure and acceleration series as well as the calculated coherence. Unnormalized transfer function boundaries of compliance signal can be obtained by the cross-correlation over the autocorrelation of pressure and acceleration series. Following Crawford et al. (1991) and Willoughby (2003), it is more appropriate to fit the regression of ground acceleration, onto pressure, which is the lower bound on compliance, because the pressure signal is stronger, independent of sedimentary structure, and less noisy than ground accelerations, which is dependent on sedimentary structure. The transfer function can be normalized by multiplying the wave number so that it is constant over a half space crust. The transfer function of OBS site S002 is plotted in the upper panel of Fig. 6. Transfer function

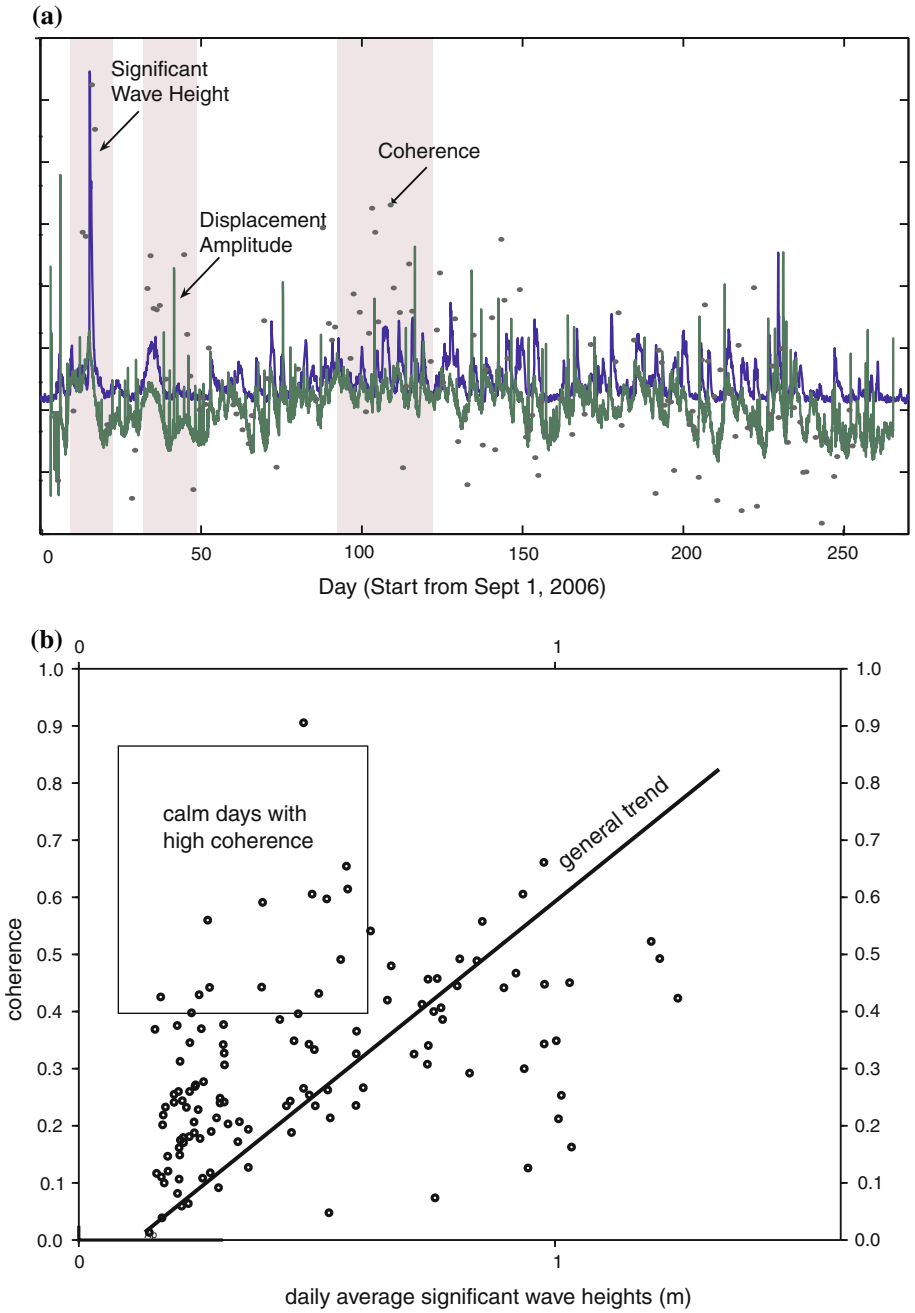

Fig. 4 **a** The correlation between significant wave heights (*blue color*) of the ocean waves, and the absolute amplitudes of the ground displacements (*green color*) recorded by the OBS at S002. We have also plotted coherence (*circles*) for comparison. The seismic data were filtered so only waves with periods longer than 12 s (mostly infra-gravity waves) were preserved. However, it is evidence that many earthquake-excited ground motions (high amplitude and short duration) can complicate the compliance studies. We found relatively good correlation among the ocean and seismic wave amplitudes and coherence. We have taken log of the seismic amplitudes and multiplied it by 2 for easier comparison to the significant wave height data, which is plotted linearly in *y* axis. The coherence is also plotted linearly in *y* axis with range between 0 at the bottom and 1.0 at the *top*. We are interested mainly on the trend, so there is no annotation for *y* axis. Overall, we found high coherences (marked inside the *light color rectangular*) when the significant wave heights are big (>1 m) or when there is more than 10 days of the medium significant wave heights (0.7–1 m). **b** Increasing significant wave heights (daily average) improve the coherence derived from OBS S002. One data point with significant wave heights greater than 1.5 m was excluded for clearer presentation, even though it also show high coherence. We have derived more than 250 coherences using daily data recorded by OBS S002. Due to the large amount of dataset, we did not exclude time windows contaminated by earthquakes. Overall there is a linear trend between significant wave heights and coherence. However, sometimes high coherence was also derived during the calm days, as shown in the *box*

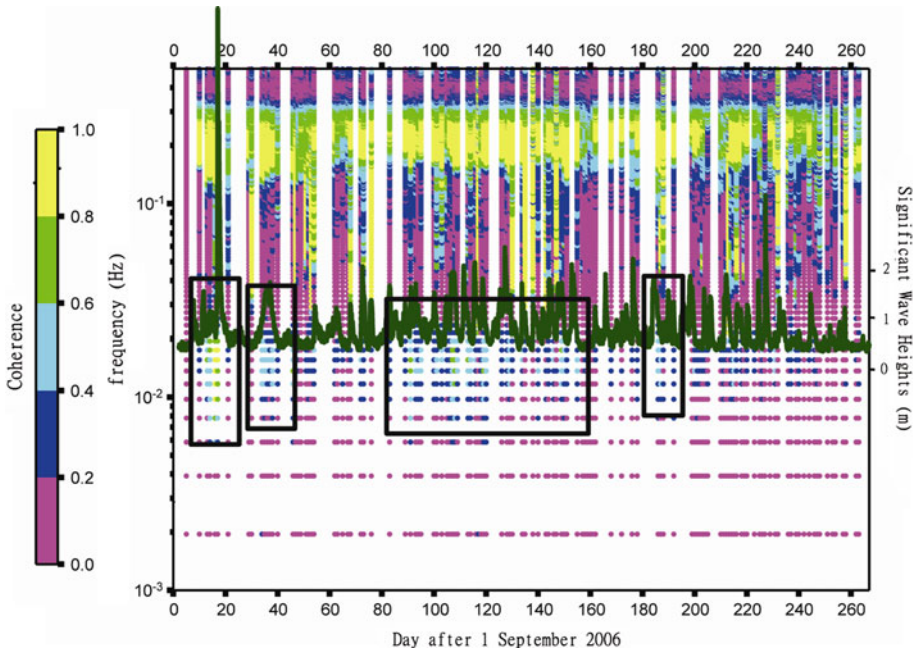

Fig. 5 Coherence functions at different frequencies during the 265 days of OBS S002 deployment. The *color bar* shows the coherence scale, with 1 being very high coherence, thus good data quality. The coherence is plotted as a function of time (*x*-axis) and frequency (*y*-axis). We are mainly focusing on the lower frequency band between 0.05 and 0.7 Hz. The thick green line is the significant wave heights. During the stormy days, the significant wave heights are large, so is the coherence in the infra-gravity bands (see the four *black boxes*)

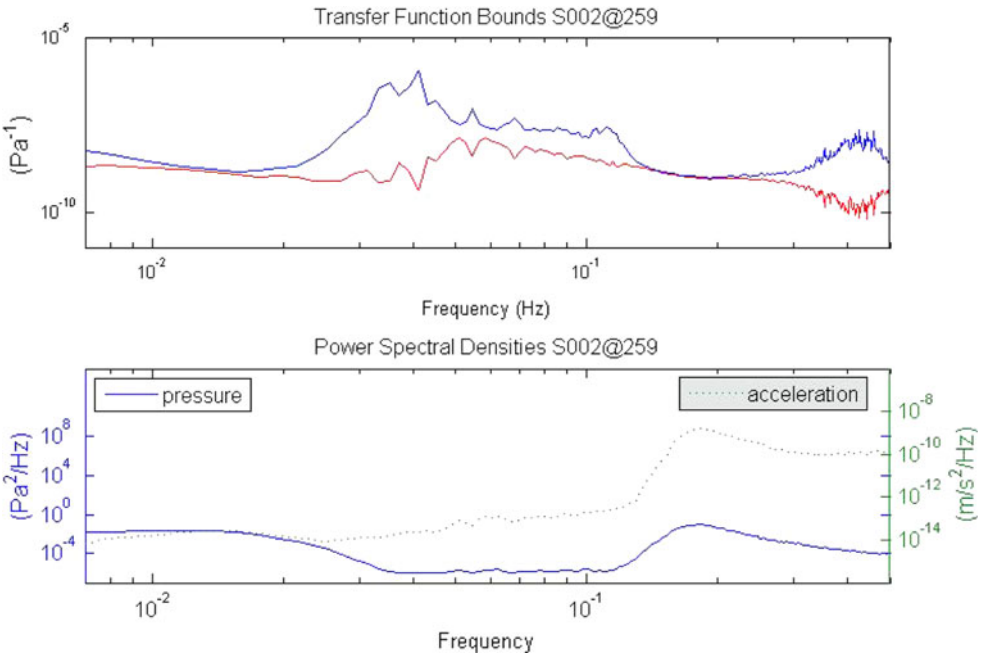

Fig. 6 The transfer functions and the power spectral densities of the pressure and acceleration data from OBS S002 on Julian day of 259 in 2006 are plotted. We have used the two power spectral densities to derive the transfer functions. The average of the two transfer functions then were used to derive a compliance curve for this site

bounds converge in the infra-gravity band and the microseimic band, and are diverge in between.

The compliance curve at S002 (Fig. 7) is obtained based on the bounds of transfer functions and the equation mentioned in previous section. We have also estimated the uncertainty bounds based on Eq. 4 of Crawford et al. (1991). The relatively tight uncertainty bounds suggest that similar studies can be conducted in hydrate regions near this site in the future where hydrates have been identified. For reference, we have also plotted synthetic compliance curves (Fig. 8) with different hydrate concentration rates for a different region.

Discussion and conclusions

Using a 10-month pressure and ground motion datasets collected on seafloor offshore Taiwan, we have developed a procedure and documented that it is possible to conduct seafloor compliance studies for gas hydrates in this region.

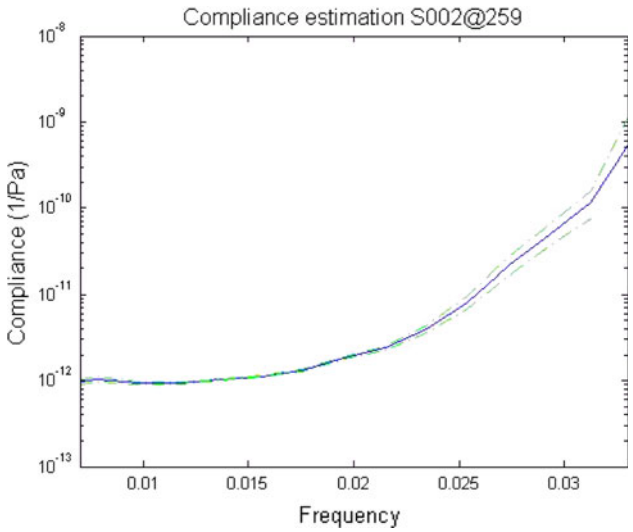

Fig. 7 Compliance curve for OBS S004 derived from the average of the two transfer functions in Fig. 5. This curved has been normalized by the wave number, as discussed in the text. We have used Eq. 4 of Crawford et al. (1991) to derive the uncertainty bounds, shown as the *dashed lines*. Due to the high coherence of the dataset, the bounds are tight

To our knowledge, this is the longest time series at stationary test sites used to investigate coherence function and seafloor compliance.

We found that the best datasets were collected during typhoons when the sea-state was rough. The relatively high significant wave heights ($\sim$3 m) induced by the typhoon probably generated a very strong forcing term, and the deformation of the seafloor acts accordingly. As a result, the signal to noise ratio is high. The coherence is relatively low when significant wave heights are lower, possibly due to contamination of storm-induced seismic signals originated from distances away from the OBSs. Actually, infragravity waves-induced ground motions are constantly excited and can travel around the global (Rhie and Romanowicz 2004, Webb et al. 1991). Such contamination might become less significant in some particular calm days when there are no storms in far distances.

A compliance curve with very high coherence has been successfully derived from this study. We propose that it is possible to study hydrates using seafloor compliance offshore Taiwan at shallow water depth using the procedure developed from this study.

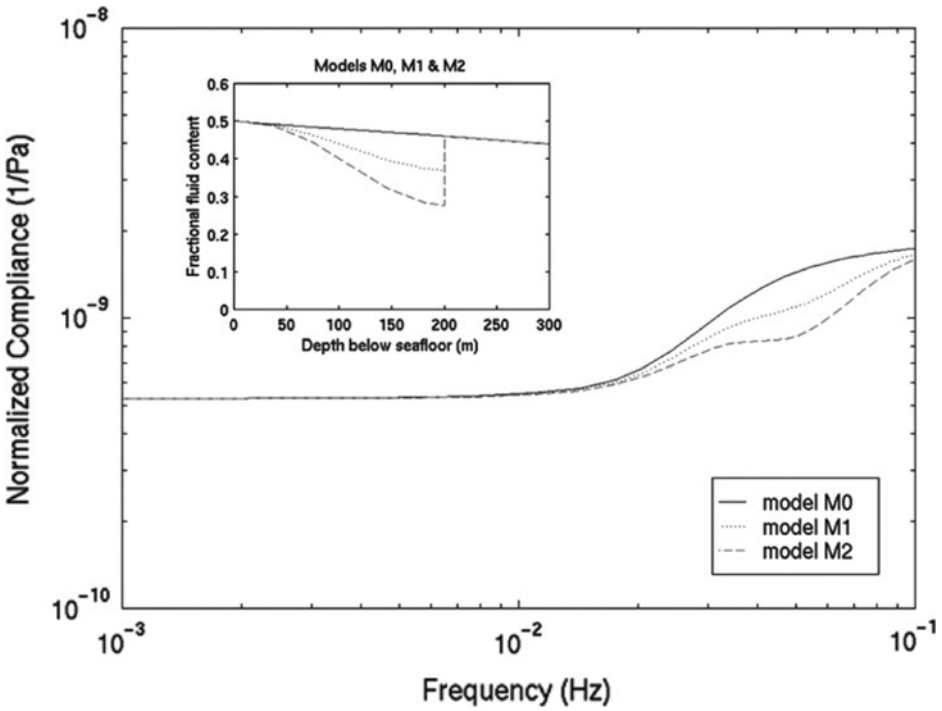

Fig. 8 Reproduced from Willoughby and Edwards (1997), who modelled the seafloor compliance response of sediments where the porosity decreases linearly with depth and there is no gas hydrate or the hydrate concentration, as a function of porosity, increases sinusoidally up to 20 and 40% of pore space, respectively, at a sharp cut-off at the phase boundary marked by the BSR. The physical parameters where selected to be typical of Northern Cascadia, offshore western Canada. There is a characteristic dip in the compliance function between 0.1 and 0.01 Hz, which increases in size as gas hydrate content is increased

Acknowledgments We thank the captain and crew members of the R/V Ocean Researcher I, who helped deploy and recover the OBSs during difficult operational environments. Central Weather Bureau of Taiwan is thanked for providing the deep sea buoy data. We thank National Institute of Informatics (NII) and Coastal Development Institute of Technology of Japan for the significant wave height and weather data. We thank two reviewers for their insightful comments, which also dramatically improve this manuscript. This research was supported by the Taiwan Earthquake Research Center (TEC) funded through National Science Council (NSC) with grant number NSC 98-2119-M-001-038. The TEC contribution number for this article is 00070. The IES contribution number is IESAS1488.

References

Chi WC, Reed DL (2008) Evolution of shallow, crustal thermal structure from subduction to collision: an example from Taiwan. GSA Bull 120:679–690

Chi WC, Reed D, Liu CS, Lundberg N (1998) Distribution of the bottom-simulating reflector in the offshore Taiwan collision zone. Terr Atmos Ocean Sci 9(4):779–794

Chi WC, Reed DL, Tsai CC (2006) Gas hydrate stability zone in offshore Southern Taiwan. Terr Atmos Ocean Sci 17:829–843

Chi WC, Chen WJ, Dolenc D, Kuo BY, Liu CR, Collins J (2010) Seismological report on the 2006 Typhoon Shanshan that lit up seismic stations along its way. Seismol Res Lett 81(4):592–596. doi: 10.1785/gssrl.81.4.592

Cox C, Deaton T, Webb S (1984) A deep-sea differential pressure gauge. J Atmo Ocean Tech 1:237–245

Crawford W (2000) Seafloor compliance measurements: applications for hydrocarbon exploration. Lithos Science Report 2:151–156

Crawford WC (2004) The sensitivity of seafloor compliance measurements to sub-basalt sediments. Geophys J Int 157: 1130–1145

Crawford WC, Singh SC (2008) Sediment shear properties from seafllor sompliance measurements: Faroes-Shetland basin case study. Geophys Prosp 56:313–325

Crawford WC, Webb SC, Hildebrand JA (1991) Seafloor compliance observed by long-period pressure and displacement measurements. J Geophys Res 96:16151–16160

Kibblewhite AC, Ewans KC (1985) Wave-wave interactions, microseisms, and infrasonic ambient noise in the ocean. J Acoust Soc Am 78(3):981–994

Kuo BY, Chi WC, Lin CR, Chang E, Collins J, Liu CS (2009) Two-station measurement of Rayleigh-wave phase velocities for the Huatung basin, the westernmost Philippine Sea, with OBS: implications for regional tectonics. Geophys J Int 179: 1859–1869. doi:10.1111/j.1365-246X.2009.04391.x

Kvenvolden KA (1988) Methane hydrate—a major reservoir of carbon in the shallow geosphere. Chem Geol 71:41–51

Kvenvolden KA (1993) Gas hydrates-geological perspective and global change. Rev Geophys 31:173–183

Kvenvolden KA, McMenamin MA (1980) Hydrates of natural gas: a review of their geological occurrences. US Geological Survey Circular 825:1–11

Lin CR, Kuo BY, Liang WT, Chi WC, Huang YC, Collins J, Wang CY (2010) Ambient noise and teleseismic signals recorded by ocean-bottom seismometers offshore eastern Taiwan. Terr Atmos Ocean Sci. doi:10.3319/TAO.2009.09.14.01(T)

Liu CS, Schnurle P, Wang Y, Chuang SH, Chen SC, Hsiuan TH (2006) Distribution and characters of gas hydrate offshore of southwestern Taiwan. Terr Atmos Ocean Sci 17:615–644

Longuet-Higgins MS, Stewart RW (1962) Radiation stress and mass transport in gravity waves, with application to surf-beats. J Flu Mech 13:481–504

McIntosh K, Nakamura Y, Wang TK, Shih RC, Chen A, Liu CS (2005) Crustal-scale seismic profiles across Taiwan and the western Philippine Sea. Tectonophysics 401:23–54

Milkov AV (2004) Global estimates of hydrate-bound gas in marine sediments: how much is really out there? Earth Sci Rev 66(3–4):183–197

Ning X, Wu SG, Wang XJ, Dong DD (2009) The characteristics of fluid potential in mud diapirs associated with gas hydrates in the Okinawa trough. Terr Atmos Ocean Sci 17:871–881

Reed DL, Lundberg N, Liu CS, Luo BY (1992) Structural relations along the margins of the offshore Taiwan accretionary wedge: implications for accretion and crustal kinematics. Acta Geol Taiwan 30:105–122

Rhie J, Romanowicz B (2004), Excitation of earth's continuous free oscillations by atmosphere-ocean-seafloor coupling. Nature 431:552–556

Shipley TH, Houston MH, Buffler RT, Shaub FJ, McMillen KJ, Ladd JW, Worzel JL (1979) Seismic evidence for widespread possible gas hydrate horizons on continental slopes and rises. AAPG Bull 63:2204–2213

Trevorrow MV, Yamamoto T, Turgut A, Goodman D, Badiey M (1989) Very low frequency ocean bottom ambient seismic noise and coupling on the shallow continental shelf. Mar Geop Res 11:129–152

Tucholke BE, Byran GM, Ewing JI (1977) Gas-hydrate horizons detected in seismic-profiles data from the western Northern Atlantic. AAPG Bull 61:698–707

Webb S (2007) The Earth's 'hum' is driven by ocean waves over the continental shelves. Nature 445. doi: 10.1038/nature05536

Webb S, Zhang X, Crawford W (1991) Infragravity waves in the deep ocean. J Geophys Res 96:2723–2736

Willoughby EC (2003) Resource evaluation of marine gas hydrate deposits using the seafloor compliance method: experimental methods and results, Ph.D. thesis, University of Toronto

Willoughby EC, Edwards RN (1997) On the resource evaluation of marine gas-hydrate deposits using seafloor compliance methods. Geophys J Int 131:751–766

Willoughby EC, Latychev K, Edwards RN, Mihajlovic G (2000) Resource evaluation of marine gas hydrate deposits using seafloor compliance methods. In: Holder GD, Bishnoi PR (eds) Gas hydrates: challenges for the future. The New York Academy of Science, New York, pp 146–158

Willoughby EC, Latychev K, Edwards RN, Schwalenberg K, Hyndman RD (2008) Seafloor compliance imaging of marine gas hydrate deposits and cold vent structures. J Geophys Res 113:B07107. doi:10.1029/2005JB004136

Yamamoto T, Torii T (1986) Seabed shear modulus profile inversion using surface gravity (water) wave-induced bottom motion. Geophys J Int 85:413–431

Yamamoto T, Trevorrow MV, Badley M, Turgut A (1989) Determination of the seabed porosity and shear modulus profiles using a gravity wave inversion. Geophys J Int 98:173–182